J. Astron. Space Sci. 23(2), 97–104 (2006)

RED GIANT BRANCH OF THE METAL POOR GLOBULAR CLUSTERS: II. BUMP, TIP, AND DISTANCE OF NGC 1904

J.-W. Kim, Y. Choi, S.-H. Chun, J. Jung, A. Kang, and Y.-J. Sohn†
Department of Astronomy, Yonsei University, Seoul 120-749, Korea
email: kjw0704@galaxy.yonsei.ac.kr

(Received April 4, 2006; Accepted May 8, 2006)

ABSTRACT

From the BV images of the metal-poor globular cluster NGC 1904 obtained with the 2K CCD camera equipped on the BOAO 1.8m telescope, we construct $(B-V, V)$ color-magnitude diagram of the cluster. The apparent V magnitudes of the RGB bump and tip have been measured from the luminosity function of the iteratively selected RGB stars in NGC 1904. Theoretical absolute M_V magnitudes of the RGB bump and tip are estimated using the Yonsei-Yale isochrones. The distance modulus of NGC 1904 has been derived by comparing the observed apparent V magnitude with the estimated absolute M_V magnitude of the RGB bump and tip.

Keywords : RGB bump, RGB tip, distance, NGC 1904, photometry

1. INTRODUCTION

NGC 1904 is a centrally concentrated metal poor globular cluster at the Galactic halo. Because of its high galactic latitude, ($b = -29°.3$), interstellar reddening and contamination by field stars are almost negligible. This has made the cluster well suited for photometric study. The first photometric studies for NGC 1904 were made by Goranskij (1976) and Alcaino (1976). Stetson & Harris (1977) published a *UBV* photographic photometry of stars in NGC 1904 and found populus blue horizontal branch stars. Harris et al. (1983) first established the location of main-sequence stars, and Heasley et al. (1986) secured the first CCD photometry of the cluster. From the wide-field photometry, Ferraro et al. (1992) obtained a deep BV photometry and confirmed the morphology of the color-magnitude diagram (CMD) in previous studies, such as a mean metallicity and the red giant bump at $V = 16.00 \pm 0.05$. Alcaino et al. (1994) presented a deep *BVRI* CCD photometry and analyzed the obtained CMD with theoretical isochrones to derive several photometric parameters. More recently, from the CCD photometry of NTT, Kravtsov et al. (1997) studied the CMD morphology of NGC 1904 and evaluated the red giant branch (RGB) bump position as $V = 15.95 \pm 0.10$. They also pointed out that the cluster has an extremely blue horizontal branch, extending as faint as the main-sequence turn-off.

In this paper, we construct the V band luminosity function (LF) of the RGB stars in NGC 1904 from the BV CCD photometry obtained with the BOAO 1.8m telescope to detect the RGB bump and tip, from which we evaluate the distance modulus of the cluster. The magnitude levels of the

†corresponding author

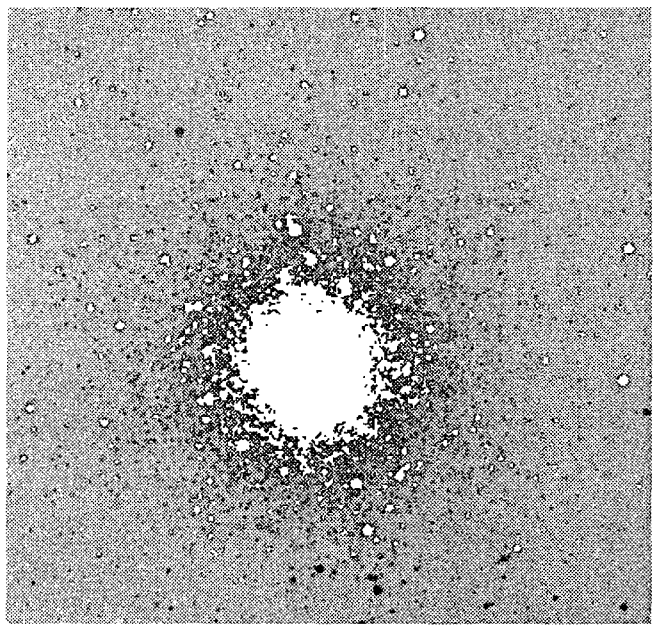

Figure 1. The reduced V image of NGC 1904. The entire field of view is 11.8 × 11.8 arcmin^2.

RGB bump and the RGB tip in a stellar system contain crucial astrophysical significance of the low-mass stellar evolution and the cosmic distance scale of the system. During the post main-sequence evolution of low mass stars at the hydrogen burning shell stage, a star experiences an evolutionary hesitation as the convective envelope penetrates deeply enough into the narrow hydrogen burning shell. This yields an RGB bump on a LF of RGB stars in a globular cluster. The RGB tip on the LF is populated by stars whose electron degenerate core is about to start the helium flash, and manifests itself as a discontinuity in the LF of RGB stars in the CMDs of globular clusters. The physical origin of the RGB bump was first pointed out by Thomas (1967) and Iben (1968), and the observation of the RGB bump from LFs has been the subject of many studies (e.g., King et al. 1985, Fusi Pecci et al. 1990, Ferraro et al. 1999, Cho & Lee 2002, Valenti et al. 2005, and references therein). The RGB tip is now considered to be a good distance indicator for stellar populations displaying an RGB in their CMDs (Lee et al. 1993, Madore & Freedman 1995, Ferrarese et al. 2000a,b, Bellazzini et al. 2001, Walker 2003, Salaris & Girardi 2005).

The observations and data reduction are described in Sec. 2. In Sec. 3, we show the $(B-V, V)$ CMD and the LF in V of stars in NGC 1904, and determine the apparent V magnitudes of the RGB bump and tip. In Sec. 4 we present the absolute M_V magnitudes of the RGB bump and tip predicted by the Yonsei-Yale isochrones. We also derive the distance modulus of NGC 1904 in Sec. 4. Results are summarized in Sec. 5.

2. OBSERVATIONS AND DATA REDUCTION

The BV images of NGC 1904 and a number of Landolt (1992) standard stars were obtained over the night of UT 2001 January 30 by using the 1.8m telescope at BOAO. The detector was SITe

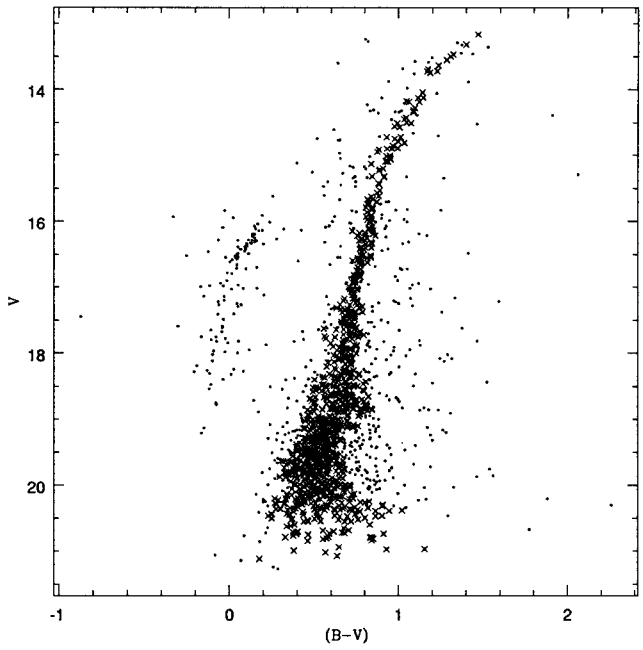

Figure 2. The $(B-V, V)$ CMD of NGC 1904. Cross-marks indicate the stars selected by 2σ rejection procedure.

CCD chip with a 2048 × 2048 format. The sky coverage of an image is 11.8 × 11.8 arcmin^2 and the image scale is 0.34 arcsec/pixel at the f/8 Cassegrain focus of the telescope. A single exposure was taken in each B and V filters with exposure times of 1,200 and 900 seconds, respectively.

The data reduction followed the standard processing line for CCD images. The bias level was removed by subtracting a master zero-level frame, and the result was divided by twilight flat images. Observations of standard stars were also secured on three fields in SA 95. Multiple aperture photometry was performed on each standard star by using the PHOTOMETRY task in the DAOPHOT II (Stetson 1987). Total magnitudes of standard stars were then calculated by applying the growth-curve analysis of the DAOGROW task (Stetson 1990). These magnitudes were corrected for the exposure time of each frame and the extinction coefficient, which was estimated from the data of time series observations of an arbitrary selected sky region. The final photometric transformations for V magnitude and $(B-V)$ color are

3. THE COLOR-MAGNITUDE DIAGRAM AND LUMINOSITY FUNCTION

The B and V magnitudes of individual stars in NGC 1904 were measured by the PSF-fitting photometry package DAOPHOTII/ALLSTAR (Stetson 1987, Stetson & Harris 1988). To calculate the PSF in each image, we used $\sim$ 50 isolated bright stars located at outer region of the cluster. An iterative method was applied to remove neighboring stars of selected PSF stars, so that we were able to achieve appropriate PSFs for each frame. Aperture correction was applied by using DAOGROW

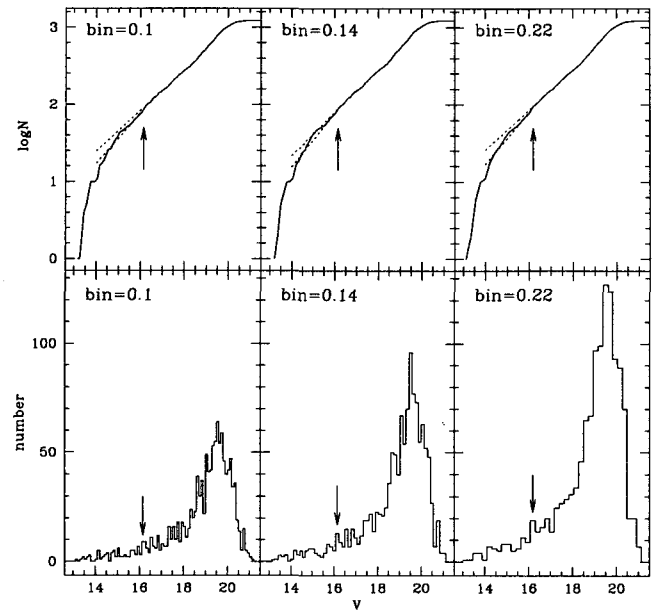

Figure 3. The differential (bottom) and integrated (top) LFs of RGB stars in NGC 1904 with various magnitude bins. Arrows indicate the RGB bump position, and the dashed lines in the integrated luminosity functions are the linear fit to the regions above and below the RGB bump.

task and the result was used to correct the measured PSF-based magnitudes for every stars in the frame. Airmass corrections and the photometric transformations were then applied to obtain the BV standard magnitude of stars.

The positional transformation to match up the coordinates of stars in B and V frame was applied by using the DAOMATCH and DAOMASTER tasks (Stetson 1992). Finally, a total of 1751 stars were detected in both B and V images of NGC 1904. Figure 2 shows the $(B-V, V)$ CMD of stars in NGC 1904. The CMD reveals a long blue tail of horizontal branch stars extending from the hotter edge of the RR Lyrae instability strip down to the level of main-sequence turn-off. The limiting magnitude extends down to $V \sim 21$ magnitudes, which is apparently ~ 1 magnitude fainter than the main-sequence turn-off.

To determine the V magnitudes of the RGB bump and tip, we construct the LF of the RGB stars in NGC 1904 following the technique in Sohn et al. (2006). First, RGB stars within a 2σ deviation of the mean color for a given magnitude bin are selected as the pure RGB sample. The procedure with a 2σ rejection criterion was then iterated until the mean values of magnitude and color are stable at constant values to avoid contamination from the other stellar populations, such as asymptotic giant branch stars and horizontal branch stars. The LF of NGC 1904 is then constructed from the selected RGB stars, and the RGB bump was defined at a significant peak in the differential LF and a corresponding slope break in the integrated LF. Figure 3 shows the LFs of RGB stars in NGC 1904 with various bins of 0.10, 0.14, and 0.22 magnitudes in V, and indicates the determined RGB bump of $V = 16.16 \pm 0.15$ magnitudes. Error in the apparent V magnitude is the mean measurement error in the LFs of a variable magnitude bin. Even when considering the measurement

Table 1. Theoretical prediction of the absolute M_V magnitude of the RGB bump and tip with respect to metallicity and age by the Yonsei-Yale isochrones.

	Bump				Tip			
[Fe/H]	7 Gyr	10 Gyr	12 Gyr	15 Gyr	7 Gyr	10 Gyr	12 Gyr	15 Gyr
0.169	1.556	1.780	1.965	2.135	1.751	1.934	1.983	2.043
-0.424	1.362	1.584	1.666	1.869	-0.805	-0.570	-0.362	0.047
-0.490	1.044	1.250	1.364	1.481	-0.980	-0.867	-0.707	-0.320
-0.650	0.831	1.055	1.156	1.279	-1.078	-1.118	-1.129	-1.036
-0.898	0.557	0.758	0.859	0.988	-1.683	-1.357	-1.232	-1.123
-1.505	-0.076	0.106	0.214	0.335	-2.553	-2.469	-2.432	-2.382
-1.904	-0.430	-0.268	-0.168	-0.060	-2.695	-2.682	-2.665	-2.646
-2.507	-0.788	-0.627	-0.536	-	-2.750	-2.774	-2.783	-2.787

error in LF, the determined V magnitude of the RGB bump seems to be slightly fainter than those of $V = 16.00$ and 15.95 given by Ferraro et al. (1992) and Kravtsov et al. (1997). The V magnitude of the RGB tip is determined by measuring the brightness of the brightest stars and a sharp cut-off occurring at the bright end of the LF of the RGB stars. The derived magnitude of the RGB tip is $V = 13.16 \pm 0.22$. Here, we simply assign the error to the measurement error on the LF with 0.22 magnitude bin because of poor statistics of brightest RGB stars in the obtained LFs.

4. ABSOLUTE MAGNITUDES OF THE RGB BUMP AND TIP, AND DISTANCE

4.1 Adopted metallicity and reddening

The metallicity of NGC 1904 has been determined by various photometric and spectroscopic observations. Alcaino et al. (1994) compiled the reported values of the cluster metallicity which cover the range $-1.78 <$ [Fe/H] < -1.42. Kravtsov et al. (1997) obtained the metallicity of [Fe/H] $= -1.76 \pm 0.20$ from the position of the RGB bump. Kraft & Ivans (2003) obtained [Fe/H] = –1.59 from the high resolution spectra of RGB stars in NGC 1904. Most recently, Fabbian et al. (2005) analyzed the high resolution spectra of horizontal branch stars and obtained the average metallicity of [Fe/H] $= -1.34 \pm 0.09$. The values of metallicity for NGC 1904 given by Zinn & West (1984) and Carreta & Gratton (1997) are [Fe/H] = –1.67 and –1.37, respectively. Considering the previously determined metallicity of NGC 1904, we use three values of [Fe/H] = –1.80, –1.56, and –1.32 for NGC 1904 to check the dependency of the absolute magnitudes of the RGB tip and bump on metallicity.

Interstellar reddening toward NGC 1904 is almost negligible because NGC 1904 is located at high galactic latitude. Alcaino et al. (1994) compiled the interstellar reddening values of NGC 1904 derived in various studies in the range of $0.00 < E(B-V) < 0.02$. In the Table of Harris (1996), the reddening value of NGC 1904 is $E(B-V) = 0.01$, which yields $A_V = 0.03$ magnitude with $A_V/E(B-V) = 3.315$ (Schlegel et al. 1998). Here we adopt this value.

4.2 The absolute M_V magnitude

The theoretical prediction of the absolute M_V magnitudes of the RGB bump and tip is estimated by the Yonsei-Yale isochrones (Kim et al. 2002, Yi et al. 2003) for the α–elements enhancement factor of 0.3. Table 1 and Figure 4 show the theoretical prediction of the M_V magnitudes of the RGB bump and tip with respect to the cluster metallicity and age. The RGB bump and tip move to

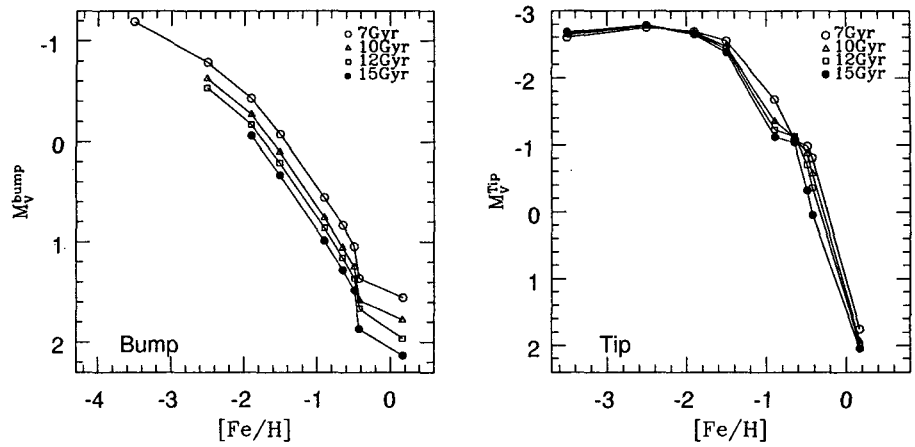

Figure 4. The absolute M_V magnitude of the RGB bump (left) and tip (right) as a function of metallicity [Fe/H] with ages of 7, 10, 12, and 15 Gyr.

fainter location with increasing cluster metallicity and age at [Fe/H] ≤ -0.8.

The absolute M_V magnitudes of the RGB bump and tip at three values of [Fe/H] = −1.80, −1.56, and −1.32 are calculated by applying the polynomial interpolation to the theoretical magnitude-metallicity planes in Figure 4 of Yonsei-Yale isochrones. Table 2 lists the estimated theoretical M_V magnitudes of the RGB bump and tip with respect to the cluster age at the given values of metallicity for NGC 1904.

4.3 Distance

The distance modulus of NGC 1904 is now directly calculated by using the observed V magnitudes of the RGB bump and tip, the adopted reddening value, and the derived absolute M_V magnitudes of the RGB bump and tip. Table 3 lists the estimated distance modulus of NGC 1904 with respect to the cluster age at three values of given metallicity. Note that errors of the calculated distance modulus of NGC 1904 in Table 3 contain only the measurement errors of the RGB bump and tip on the LF of the selected RGB stars, i.e. 0.15 and 0.22 magnitudes, respectively. It is apparent in Table 3 that the cases of [Fe/H] = −1.56 in the same age and age = 15 Gyr in the same metallicity show the smallest discrepancy between the distances estimated from the RGB bump and tip. The difference between the distance moduli from the RGB bump and tip for the case of 15 Gyr and [Fe/H] = −1.56 is 0.28 magnitude. Meanwhile, the average distance modulus of NGC 1904 is calculated as 15.96 ± 0.22 from the RGB bump and 15.52 ± 0.24 from the RGB tip, considering only three cases of ages, 10, 12, and 15 Gyrs except for 7 Gyr. We cautiously attribute this discrepancy of 0.44 magnitude to the ambiguity of measurement of the RGB tip on the observed CMD by the poor statistics of the brightest stars around the RGB tip, and the definition of the RGB tip from theoretical isochrone as well, rather than the RGB bump. We therefore assign the distance modulus of NGC 1904 as 15.85 ± 0.15 by adopting the case of 15 Gyr and [Fe/H] = −1.56 for the RGB bump in Table 3.

Here, we compare the distance modulus of NGC 1904 with the previous determinations. Ferraro et al. (1992) determined the distance modulus of NGC 1904 to be 15.45 ± 0.02 and a solar distance

Table 2. Theoretical prediction of the absolute M_V magnitude of the RGB bump and tip with respect to the cluster age at the values of [Fe/H] = –1.80, –1.56, and –1.32.

	Bump				Tip			
[Fe/H]	7 Gyr	10 Gyr	12 Gyr	15 Gyr	7 Gyr	10 Gyr	12 Gyr	15 Gyr
-1.80	-0.338	-0.171	-0.069	0.043	-2.677	-2.651	-2.630	-2.604
-1.56	-0.125	0.055	0.160	0.280	-2.587	-2.516	-2.482	-2.437
-1.32	0.117	0.305	0.410	0.534	-2.376	-2.145	-2.056	-1.981

Table 3. The estimated distance modulus of NGC 1904 with respect to the cluster age at the values of [Fe/H] = –1.80, –1.56, and –1.32.

	Bump				Tip			
[Fe/H]	7 Gyr	10 Gyr	12 Gyr	15 Gyr	7 Gyr	10 Gyr	12 Gyr	15 Gyr
-1.80	16.47	16.30	16.20	16.09	15.81	15.78	15.76	15.73
-1.56	16.25	16.08	15.97	15.85	15.72	15.65	15.61	15.57
-1.32	16.01	15.83	15.72	15.60	15.51	15.28	15.19	15.11

of 12 ± 2 Kpc using the observed magnitudes of the main sequence turn-off and horizontal branch from the combined photographic and BV CCD photometry. Alcaino et al. (1994) compared the *BVRI* photometry of stars in NGC 1904 with the isochrones (VandenBerg & Bell 1985) to derive the distance modulus of NGC 1904 as 15.75 ± 0.01. Kravtsov et al. (1997) also presented that the 18 Gyr VandenBerg & Bell (1985) isochrone for [Fe/H] = –1.78 shows the best fit for the distance modulus of 15.75 to the obtained CMD. From the matching of the magnitude of the horizontal branch and the theoretical models (Straniero et al. 1997), Ferraro et al. (1999) provide the distance modulus of NGC 1904 as 15.63. In the Table of Harris (1996), the distance modulus of NGC 1904 is 15.59. In summary, the previously determined distance modulus of NGC 1904 are in the range of 15.45 $\sim$ 15.75. We therefore conclude that the distance modulus estimated in this paper, i.e. 15.85 ± 0.15, is slightly larger than those of previous measurements. This indicates that further accurate calibrations for the distance measurements from the RGB bump and the other methods are needed from the photometric and theoretical analyses on the RGB bump.

5. SUMMARY

The $(B - V, V)$ CMD of stars in the metal poor globular cluster NGC 1904 has been derived from the BV images which were obtained by using 2K CCD camera and the BOAO 1.8m telescope. We constructed the LF of the RGB stars and measured the apparent V magnitudes of the RGB bump and tip. Theoretical absolute M_V magnitudes of the RGB bump and tip are also estimated by the prediction of the Yonsei-Yale isochrones. By comparing the observed V magnitude and the theoretical M_V magnitude of the RGB bump, we derived the distance modulus of NGC 1904 is 15.85 ± 0.15 for the case of 15 Gyr and [Fe/H]= −1.56. Further accurate calibrations for the distance measurements from the RGB bump has been suggested.

ACKNOWLEDGEMENTS: This work was supported by the Korea Research Foundation Grant funded by the Korean Government (KRF-2005-003-C00083), for which we are grateful.

REFERENCES

Alcaino, G. 1976, A&AS, 26, 353
Alcaino, G., Liller, W., Alvarado, F., & Wenderoth, E. 1994, AJ, 107, 230
Bellazzini, M., Ferraro, F. R., & Pancino, E. 2001, ApJ, 556, 635
Carreta, E. & Gratton, R. G. 1997, A&AS, 121, 95
Cho, D. -H. & Lee, S. -G. 2002, AJ, 124, 977
Fabbian, D., Recio-Blanco, A., Gratton, R. G., & Piotto, G. 2005, A&A, 434, 235
Ferrarese, L., Ford, H. C., Huchra, J., Kennicutt, R. C., Mould, J. R., Sakai, S., Freedman, W. L., Stetson, P. B., Madore, B. F., Gibson, B. K., Graham, J. A., Hughes, S. M., Illingworth, G. D., Kelson, D. D., Macri, L., Sebo, K., & Silbermann, N.A. 2000a, ApJS, 128, 431
Ferrarese, L., Mould, J. R., Kennicutt, R. C., Huchra, J., Ford, H. C., Freedman, W. L., Stetson, P. B., Madore, B. F., Sakai, S., Gibson, B. K., Graham, J. A., Hughes, S. M., Illingworth, G. D., Kelson, D. D., Macri, L., Sebo, K., & Silbermann, N.A. 2000b, ApJ, 529, 745
Ferraro, F. R., Clementini, G., Fusi Pecci, F., Sortino, R., & Buonanno, R. 1992, MNRAS, 256, 391
Ferraro, F. R., Messineo, M., Fusi Pecci, F., De Palo, M. A., Straniero, O., Chieffi, A., & Limongi, M. 1999, AJ, 118, 1738
Fusi Pecci, F., Ferraro, F. R., Crocker, D. A., Rood, R. T., & Buonanno, R. 1990, A&A, 238, 95
Goranskij, V. P. 1976, Astr. Tsirk., 902, 5
Harris, W. E. 1996, AJ, 112, 1487
Harris, W. E., Hesser, J. E., & Atwood, B. 1983, PASP, 95, 951
Heasley, J. N., Janes, K. A., & Christian, C. A. 1986, AJ, 91, 1108
Iben, I. Jr. 1968, Nature, 220, 143
Kim, Y. -C., Demarque, P., Yi, S. K., & Alexander, D. R. 2002, ApJS, 143, 499
King, C. R., Da Costa, G. S., & Demarque, P. 1985, ApJ, 299, 674
Kraft, R. P. & Ivans, I. I. 2003, PASP, 115, 143
Kravtsov, V., Ipatov, A., Samus, N., Alcaino, G., Liller, W., & Alvarado, F. 1997, A&AS, 125, 1
Landolt, A. U. 1992, AJ, 104, 340
Lee, M. G., Freedman, W. L., & Madore, B. F. 1993, ApJ, 417, 553
Madore, B. F. & Freedman, W. L. 1995, AJ, 109, 1645
Salaris, M. & Girardi, L. 2005, MNRAS, 357, 669
Schlegel, D. J., Finkbeiner, D. P., & Davis, M. 1998, ApJ, 500, 525
Sohn, Y. -J., Kim, J. -W., & Kang, A. 2006, submitted to JA&SS
Stetson, P. B. 1987, PASP, 99, 191
Stetson, P. B. 1990, PASP, 102, 932
Stetson, P. B. 1992, in IAU Colloq. 136, Stellar Photometry: Current Techniques and Future Developments, eds. C. J. Butler & I. Elliot (Cambridge: Cambridge Univ. Press), p.291
Stetson, P. B. & Harris, W. E. 1977, AJ, 82, 954
Stetson, P. B. & Harris, W. E. 1988, AJ, 96, 909
Straniero, O., Chieffi, A., & Limongi, M. 1997, ApJ, 490, 425
Thomas, H. -C. 1967, Z. Astrophys., 67, 420
Valenti, E., Origlia, L., & Ferraro, F. R. 2005, MNRAS, 361, 272
VandenBerg, D. A. & Bell, R. A. 1985, ApJS, 58, 561
Walker, A. R. 2003, in Stellar candles for the extragalactic distance scale, eds. D. Alloin, & W. Gieren (New York: Springer), Lect. Notes Phys., 635, 265
Yi, S. K., Kim, Y. -C., & Demarque, P. 2003, ApJS, 144, 259
Zinn, R. & West, M. J. 1984, ApJS, 55, 45